Research Article

Meteorological Factors Affecting Winter Particulate Air Pollution in Ulaanbaatar from 2008 to 2016

Minrui Wang[1),2),*], **Kenji Kai**[1),3)], **Nobuo Sugimoto**[4)], **Sarangerel Enkhmaa**[5)]

[1)]Graduate School of Environmental Studies, Nagoya University, D2-1(510) Furo-cho, Nagoya, Aichi 464-8601, Japan
[2)]Institute for Space-Earth Environmental Research, Nagoya University, Furo-cho, Nagoya, Aichi 464-8601, Japan
[3)]College of Education, Ibaraki University, 2-1-1, Bunkyo, Mito, Ibaraki 310-8512, Japan
[4)]National Institutes for Environmental Studies, 16-2 Onogawa, Tsukuba, Ibaraki 305-0053, Japan
[5)]Government Implementing Agency for Meteorology & Environmental Monitoring, Juulchin street-5, Ulaanbaatar-15160, Mongolia

*Corresponding author.
Tel: +81-52-747-6414
E-mail: wang.minrui@g.mbox.nagoya-u.ac.jp

Received: 26 January 2018
Revised: 7 June 2018
Accepted: 15 June 2018

ABSTRACT   Ulaanbaatar, the capital of Mongolia, is subject to high levels of atmospheric pollution during winter, which severely threatens the health of the population. By analyzing surface meteorological data, ground-based LIDAR data, and radiosonde data collected from 2008 to 2016, we studied seasonal variations in particulate matter (PM) concentration, visibility, relative humidity, temperature inversion layer thickness, and temperature inversion intensity. PM concentrations started to exceed the 24-h average standard ($50\,\mu g/m^3$) in mid-October and peaked from December to January. Visibility showed a significant negative correlation with PM concentration. Relative humidity was within the range of 60-80% when there were high PM concentrations. Both temperature inversion layer thickness and intensity reached maxima in January and showed similar seasonal variations with respect to PM concentration. The monthly average temperature inversion intensity showed a strong positive correlation with the monthly average $PM_{2.5}$ concentration. Furthermore, the temperature inversion layer thickness exceeded 500 m in midwinter and overlaid the weak mixed layer during daytime. Radiative cooling enhanced by the basin-like terrain led to a stable urban atmosphere, which strengthened particulate air pollution.

KEY WORDS   LIDAR, Mixed layer, Radiosonde, Temperature inversion layer, $PM_{2.5}$

1. INTRODUCTION

Since the dissolution of the Soviet Union in the 1990s, Ulaanbaatar, the capital of Mongolia, has grown rapidly. Both population and urban functions are intensely concentrated in Ulaanbaatar (World Bank, 2010). The population of Ulaanbaatar exceeded 1.3 million in 2016, accounting for ~50% of the Mongolian population. The rapid growth of the population without the addition of sufficient urban infrastructure has caused both social and environmental problems (World Bank, 2009). Atmospheric pollution in winter is one of the most serious environmental problems threatening the health of its citizens, and has affected infant mortality in the last 10-15 years (Oyunchimeg and Burmaa, 2005).

Among cities that experience atmospheric pollution episodes, Ulaanbaatar is at a much higher latitude and experiences longer and colder winters. Moreover, as an inland city, Ulaanbaatar has unique topographic and geographic characteristics that
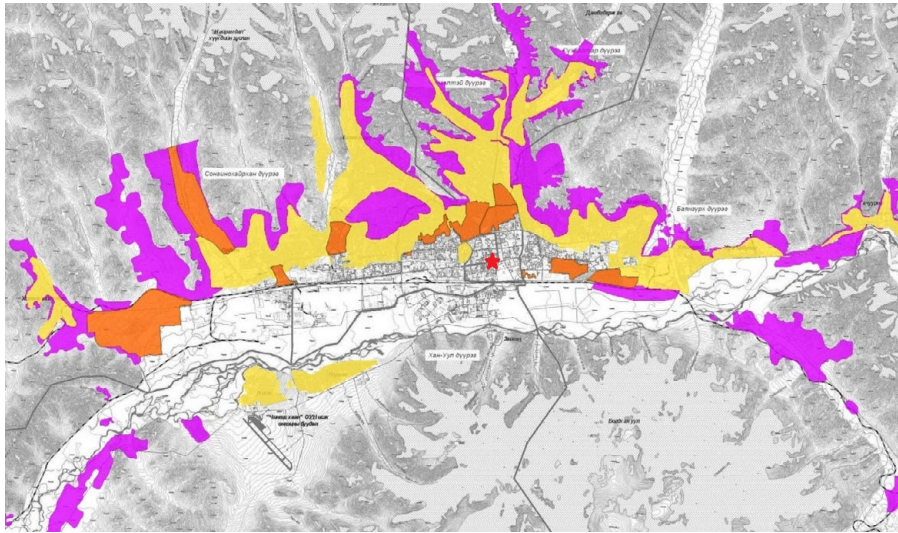
Fig. 1. Map showing the distribution of the main urban area, central ger districts (orange zone), middle ger districts (yellow zone), and fringe ger districts (purple zone) in Ulaanbaatar. The red star indicates the location of the observation site (modified from Enkhbayar, 2014).

provide suitable conditions for the formation of thick inversion layers in winter. Ulaanbaatar is located in a basin surrounded by mountains to the north and south, and the narrow urban area extends from east to west between the mountains (Fig. 1). Ger districts, consisting of gers (traditional Mongolian dwellings) and other dwellings made of brick or wood, are distributed mainly in the northern valleys and western suburbs around the urban area. These ger districts are considered to be the main source of particulate matter (PM) emissions in Ulaanbaatar. The number of gers and households in ger districts decreased from 1992 to 1996 due to the chaotic economy after the dissolution of the Soviet Union. However, an increasing number of people moved to the suburbs of Ulaanbaatar after 1997. This was driven in part by the urbanization of Ulaanbaatar, which provided more jobs and a better educational environment, as well as an increase in natural disasters (such as dzud in winter) in steppe and meadow areas, resulting in an explosive increase from 1997 to 2005. With the increasing population and number of gers, ger districts have spread over an increasingly wide area (Matsumiya, 2015; Amarsaikhan *et al.*, 2009).

Vehicles represent another source of air pollutants and major threat to air quality in Ulaanbaatar. They influence the urban atmosphere not only via exhaust, but by disturbing soil and creating floating dust along roads, especially unpaved roads. Both the total number

of vehicles and number of private cars have increased significantly in the past 25 years, most of which are used. Before 2005, approximately 74% of the vehicles in Ulaanbaatar were more than seven years old and 80% did not meet fuel consumption or emission standards (Nyamtseren, 2009; Abres *et al.*, 2006). This has not changed in the past ten years, and the city government had to enact decrees to circumscribe the number of active vehicles by license number.

Although the problems caused by vehicles persist throughout the year, severe particulate air pollution in Ulaanbaatar only occurs in winter. Therefore, researchers and government officials must identify the main sources and formation mechanism of particulate air pollution to mitigate this problem. In our previous work, we clarified the occurrence of pollution, diurnal variation of wind, and seasonal variation in the atmospheric boundary layer in Ulaanbaatar in 2010 (Wang *et al.*, 2017). However, the generalizability of the suppressed winter mixed layer with highly concentrated air pollutants capped by a thicker temperature inversion layer must be determined. Therefore, in this study, we investigated the seasonal variations in PM up to 2.5 μm in diameter ($PM_{2.5}$), visibility, and temperature inversion by analyzing meteorological and radiosonde data. Furthermore, we compared the temperature inversion layer thickness and diurnal mixed layer height by analyzing National Institutes for Environmental Studies

(NIES, Tsukuba, Japan) LIDAR data. This study aims to provide a scientific basis for understanding the unique characteristics of Ulaanbaatar and their effects on urban particulate air pollution in winter.

2. DATA AND METHODS

2.1 Kosa Monitor, Radiosonde and Surface Meteorological Data

Surface $PM_{2.5}$ and PM_{10} (PM up to 10 μm in diameter) data for Ulaanbaatar were collected with two aerosol monitors (E-SAMPLER; Met One Instruments, Inc., Rowlett, TX, USA) placed on top of the National Agency for Meteorology and Environment Monitoring of Mongolia (NAMEM) building as part of the Kosa monitor, which has been used in previous studies (Nishikawa *et al.*, 2011). In addition to $PM_{2.5}$ and PM_{10} data, the monitor also provides wind speed and direction and hourly visibility data (since March 2008). Because some PM_{10} data were missing from 2014 to 2016 due to a lack of maintenance, we chose March 2008 to April 2014 as the PM and visibility time series period.

The pressure, temperature, potential temperature, and wind direction in Ulaanbaatar were measured using a radiosonde at 47.9167°N and 106.8667°E at 00:00 and 12:00 UTC daily. The surface elevation of the location with a free radiosonde setting is 1313 m and the pressure at ground level usually ranges from 860 to 870 hPa. Both the radiosonde and surface meteorological data were measured at the Ulaanbaatar Meteorological Observatory and provided by NAMEM.

2.2 Temperature Inversion Layer Thickness and Intensity Calculation

Our previous studies indicated that the urban inversion layer prevails throughout the day at sufficiently low surface air temperatures and relatively stable atmospheric conditions. To determine the inversion layer thickness, we checked the radiosonde data collected at 00:00 UTC (08:00 local standard time) and identified the temperature inversions.

To calculate the height from the pressure, we used a function derived from the hydrostatic equilibrium function $dp = -\rho g dz$ and the state equation of ideal gas $p = \rho RT$:

$$\frac{dp}{p} = -\frac{gdz}{RT},$$

from the temperature lapse rate $\gamma = 0.0065 K/m$, we get $T = T_0 - \gamma z$, yielding

$$\frac{dp}{p} = -gdz/R(T_0 - \gamma z).$$

Assuming that if $z = 0$ then $p = P_0$, and if $z = h$ then $p = P$, by integrating the function through $[0, h]$, we finally obtain

$$P = P_0\left(1 - \frac{\gamma z}{T_0}\right)^{g}/(R\gamma).$$

After inserting the value of constants and changing $T_K = T_C + 273.15$, we obtain

$$P = P_0\left(1 - \frac{0.0065h}{T_0 + 273.15}\right)^{5.257}$$

$$T = T_0 + 0.0065h.$$

Finally, we obtain the function we used in this study:

$$\Delta h = \frac{\left(\left(\frac{P_0}{P}\right)^{\frac{1}{5.257}} - 1\right) \times (T + 273.15)}{0.0065} - h_0,$$

where P_0 is the sea level pressure (1013.25 hPa), h_0 is the surface elevation (1313 m), and P and T are the measured pressure and temperature at a specified height, respectively.

Days without temperature inversions or on which it did not start at ground level were excluded. In addition, if there were more than two layers of temperature inversion, the one starting from the ground level was recognized as the temperature inversion layer.

The temperature inversion layer is thicker than the diurnal mixed layer during winter in Ulaanbaatar. Since the monthly average surface inversion layer thickness calculated from our data does not exceeded 800 m, the height used to definite the temperature inversion intensity is also below 800 m. In our study, the temperature inversion intensity for all data with a valid temperature inversion layer thickness was defined as the quotient of the temperature inversion ΔT and the height at which the measured pressure was around 800 hPa (Δh_{800}),
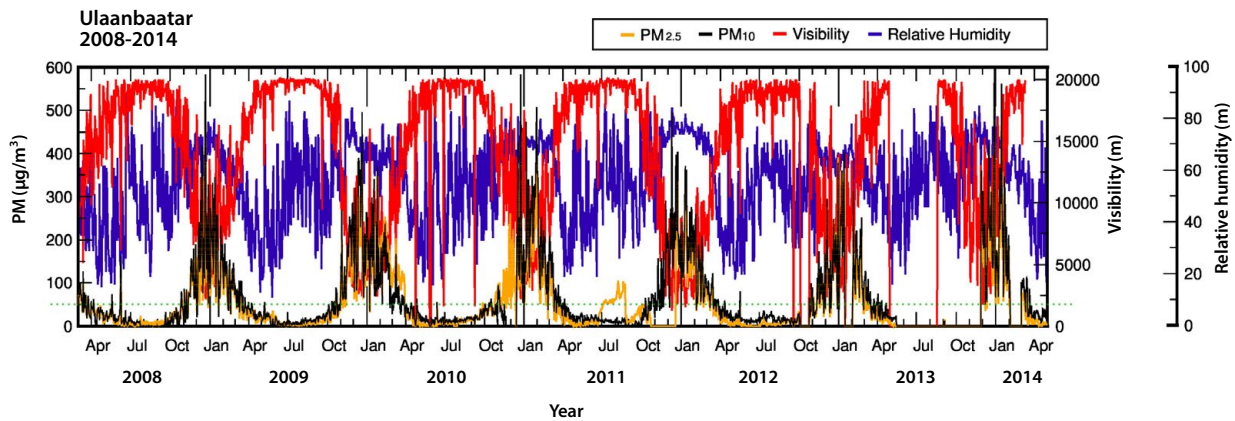
Fig. 2. Time series of the daily average $PM_{2.5}$ (orange), PM_{10} (black), visibility (red), and relative humidity (dark blue) from March 2008 to April 2014. The green dotted line represents the 24-h average standard air pollution ($50\,\mu g/m^3$) in Mongolia.

which was usually 500-600 m.

2.3 NIES LIDAR

To inspect the stability of the urban winter atmosphere, the NIES AD-net Mie-scattering LIDAR (Sugimoto *et al.*, 2009) in the center of Ulaanbaatar was used. To discuss the diurnal development of the mixed and temperature inversion layers, we used the wavelet covariance transform method to define the mixed layer height based on the LIDAR profile. Details can be found in our previous work (Wang *et al.*, 2017).

3. RESULTS

3.1 Seasonal Variations in PM, Visibility, and Relative Humidity

The daily average $PM_{2.5}$, PM_{10}, visibility, and relative humidity (RH) from March 2008 to April 2014 are shown in Fig. 2. All parameters showed significant seasonal variations. In the summer months (May-August), both $PM_{2.5}$ and PM_{10} remained below the standard ($< 50\,\mu g/m^3$; see blue line in Fig. 2) and visibility remained high (maximum: 20,000 m). When $PM_{2.5}$ and PM_{10} began to exceed the 24-h average standard of 50 $\mu g/m^3$ in October, the visibility started to decrease. The maximum $PM_{2.5}$ and PM_{10} and minimum visibility (~2500 m) were measured between December and January. The RH decreased below 40% every spring (April-June), and surpassed 60% in summer and winter. The maximum RH in 2008, 2009, 2010, 2011, and 2013 exceeded 80%, which occurred in summer (July-September). Although some data were missing because
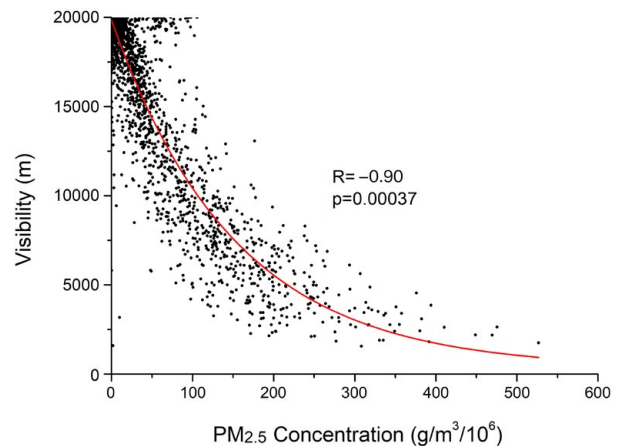

Fig. 3. Correlation between visibility and $PM_{2.5}$ concentration from March 2008 to April 2014.

of a lack of measurements, a clear negative correlation between the variations in PM and visibility was observed. For instance, there was a strong (correlation coefficient: -0.90) significant ($p = 0.00037$) correlation between visibility and $PM_{2.5}$ concentration from March 2008 to April 2014 (Fig. 3).

3.2 Seasonal Variation in the Temperature Inversion Layer

Fig. 4 shows the vertical profile of the monthly average temperature in Ulaanbaatar during the four annual seasons. In January 2008, a temperature inversion from the surface to the height at which the pressure was about 815 hPa was observed, indicating that the monthly average thickness of the temperature inversion layer was ~550 m (Fig. 4a). The temperature inversion was more than
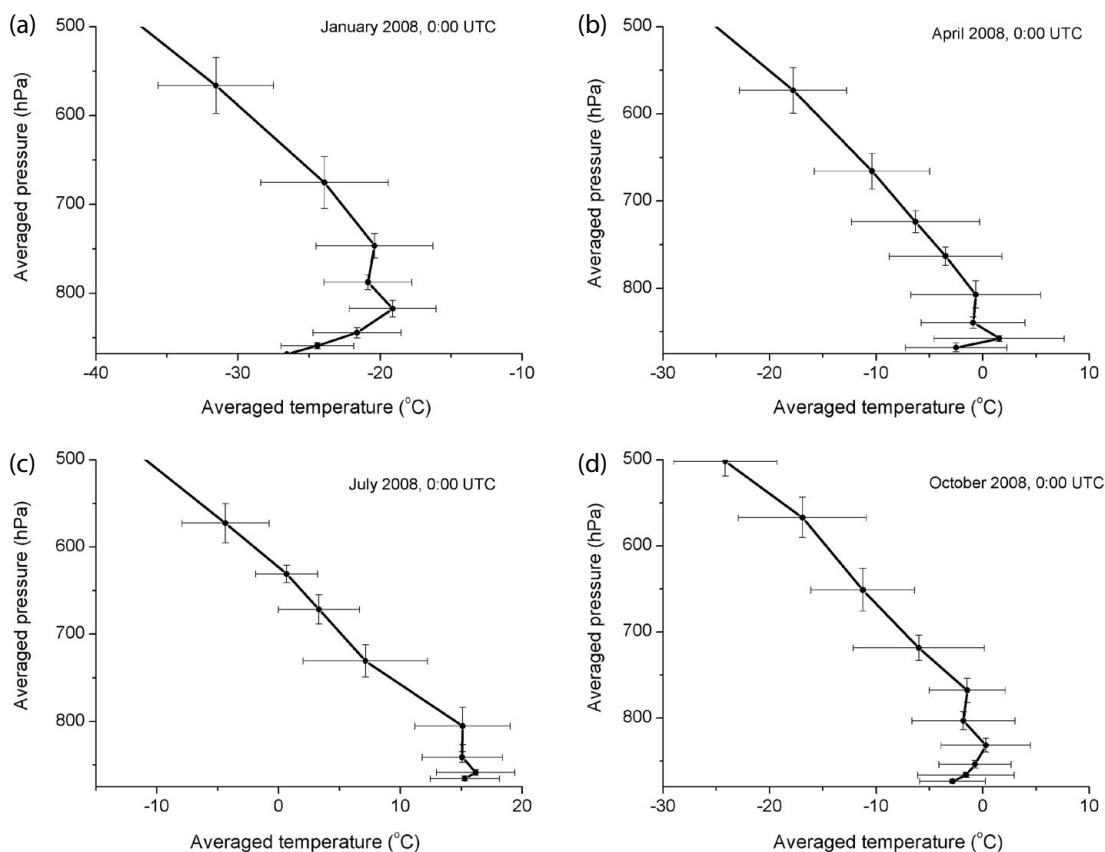
Fig. 4. Vertical profile of the monthly mean air temperature measured at 00:00 UTC (08:00 LST) in (a) January 2008, (b) April 2008, (c) July 2008, and (d) October 2008
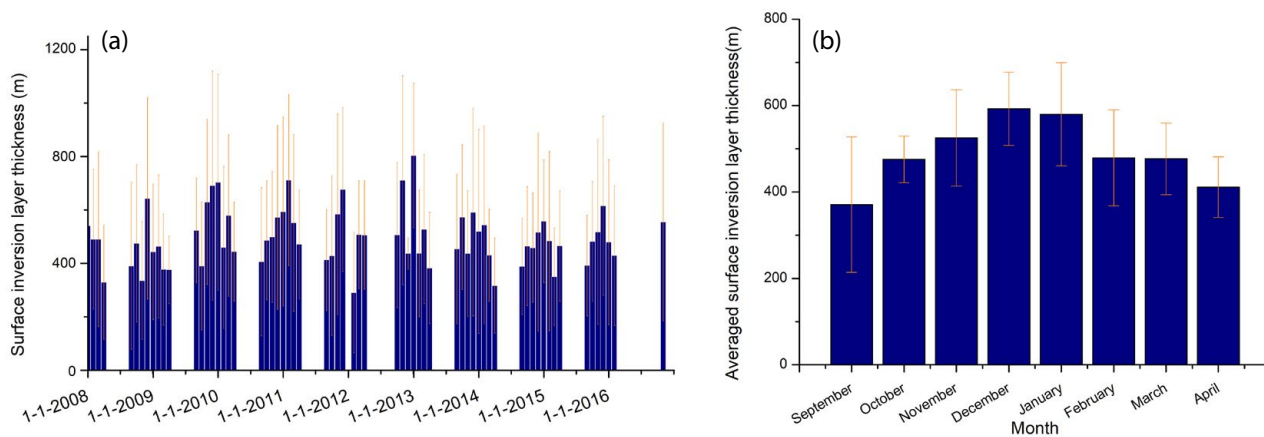

Fig. 5. (a) Time series of the monthly mean temperature inversion layer thickness (navy column) from January 2008 to December 2016. (b) Temperature inversion layer thickness (navy column) from September to April, using data averaged from 2008 to 2016. The error bars (orange) represent the standard deviation of each month.

10°C, indicating that the atmosphere was very stable. Conversely, there was no temperature inversion in summer (e.g., July 2010) (Fig. 4c). During spring and autumn, the temperature inversion was relatively weak (Fig. 4b and d), with an inversion layer thickness less than 100 m and inversion intensity below 5°C. Thus,

Table 1. Monthly mean temperature inversion (ΔT), temperature inversion layer thickness (Δh), and temperature inversion intensity between the ground level and height at 800 hPa (500-600 m) $\left(\frac{\Delta T_{800}}{\Delta h_{800}}\right)$ PM$_{2.5}$, PM$_{10}$, and visibility by month from September to April, 2008-2016.

	Sep.	Oct.	Nov.	Dec.	Jan.	Feb.	Mar.	Apr.	Avg.
ΔT (°C)	3.6	4.4	5.5	8.0	7.9	6.1	4.9	3.2	5.4
Δh (m)	371	476	525	593	580	479	477	411	489
$\frac{\Delta T_{800}}{\Delta h_{800}}$ (°C/m)	0.008	0.009	0.011	0.012	0.013	0.012	0.011	0.007	0.011
PM$_{2.5}$ (µg/m^3)	15	56	123	187	175	110	60	19	93
PM$_{10}$ (µg/m^3)	17	71	135	213	209	133	69	28	110
Visibility (km)	19.1	16.7	10.2	8.6	7.6	10.3	14.5	17.6	13.1

Table 2. Comparison of the PM$_{2.5}$ concentrations and PM$_{2.5}$/PM$_{10}$ ratios in Ulaanbaatar, Beijing, and Shanghai. The data for Beijing and Shanghai were taken from Yonemochi *et al.* (2013) and Wang *et al.* (2013), respectively. All time periods of the data from Ulaanbaatar in this table are the same as described in the text.

	Ulaanbaatar	Beijing
January 9, 2013-January 11, 2013	253 µg/m^3	249 µg/m^3
January 11, 2013-January 14, 2013	353 µg/m^3	364 µg/m^3
Maximum	766 µg/m^3 (1/13/2013, 15:00 LST)	868 µg/m^3 (1/12/2013, temporary)
	Ulaanbaatar	Baoshan district, Shanghai
December 2009-February 2010	171 µg/m^3	168 µg/m^3
PM$_{2.5}$/PM$_{10}$ ratio	0.85	0.62

the urban atmosphere in Ulaanbaatar exhibits significant seasonality, which could be confirmed with the radiosonde data.

After calculating the monthly inversion layer thickness from the radiosonde data, we determined that the temperature inversion layer in Ulaanbaatar appeared in late September and lasted until the following early April. For the months of May to August, no temperature inversions occurred. This can be exemplified by the time series of the monthly mean temperature inversion layer height from 2008 to 2016 (Fig. 5a). Every year, the seasonal variation showed the same trend, with a maximum in December or January. The temperature inversion layer thickness increased until 2013 than after 2014. Based on the monthly mean data in Fig. 5a, we furthermore averaged the data of every September, October, …, April to elucidate the seasonal variation more clearly (Fig. 5b). Although the maximum appeared in December, the value for January highly similar as that in December. Overall, both the temperature inversion (ΔT) and inversion intensity $\left(\frac{\Delta T_{800}}{\Delta h_{800}}\right)$ showed significant seasonal variations, with the averaged value of temperature inversion exceeded 6°C and the averaged inversion intensity exceeded 0.011°C/m in December, January

and February, and the values of all parameters reached the extremum during the period between December and January (Table 1). This seasonal variation had a strong influence on the surface particulate air pollution, as discussed in section 4.

4. DISCUSSION

Studies have shown that particulate air pollutants in Ulaanbaatar mainly originate from coal combustion in ger districts distributed predominantly on the northern and western sides of the city (Guttikunda, 2007), as coal combustion in domestic stoves is commonly used for residential heating. Therefore, emissions increased rapidly when the daily averaged surface temperature dropped below 0°C after mid-October. The variations in PM concentrations in this study match the results of several previous studies (Davy *et al.*, 2011; Nishikawa *et al.*, 2011). In a comparison with other studies (Yonemochi *et al.*, 2013; Wang *et al.*, 2013), the PM$_{2.5}$ and PM$_{10}$ concentrations in Ulaanbaatar were similar to those of highly polluted cities such as Beijing and Shanghai, China (Table 2), underlining the severity of winter particulate air pollution in Ulaanbaatar.
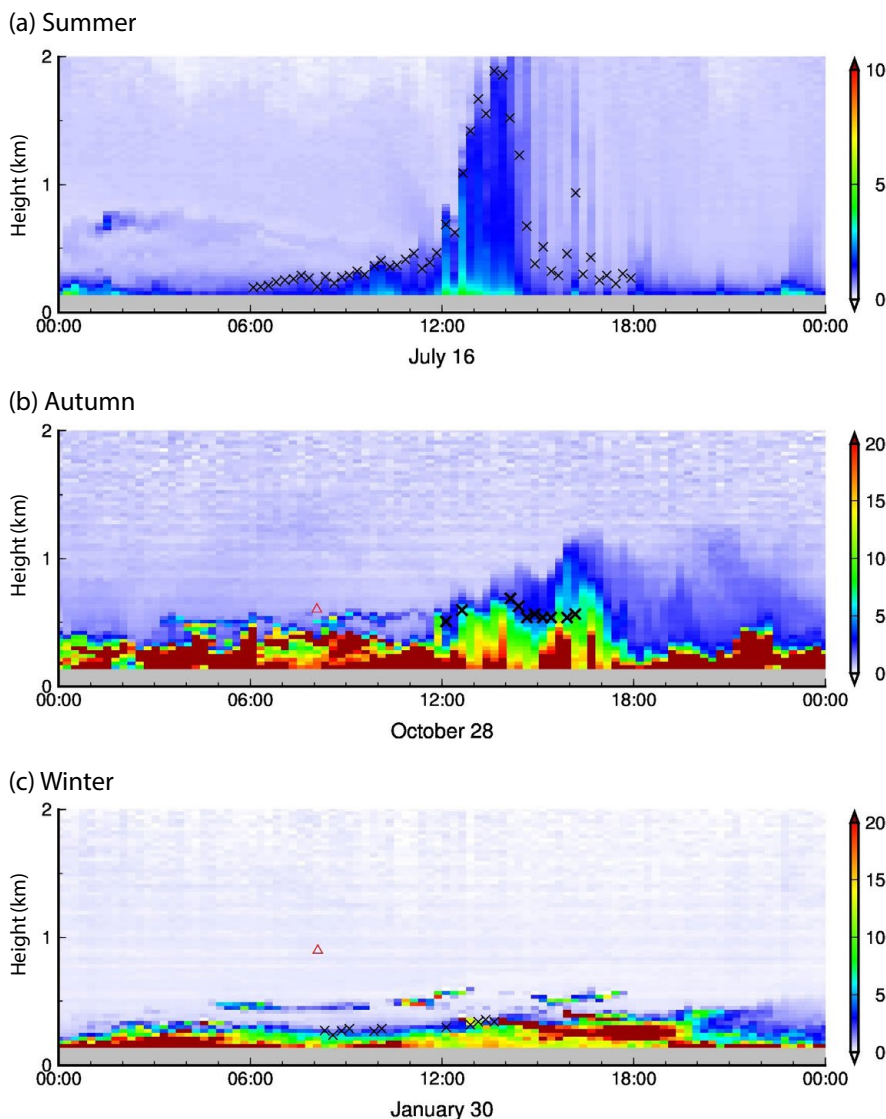
Fig. 6. Typical sunny days in three seasons on (a) July 16, 2011, (b) October 28, 2010, and (c) January 30, 2011, with the mixed layer height (black cross mark) defined from LIDAR profiles and temperature inversion layer height (red triangle) defined from radiosonde data at 08:00 LST. Color bars in three panels show the attenuated backscattering coefficient ($\times 10^{-6}$/m/sr).

As an inland city, Ulaanbaatar experiences a typical continental climate. Most precipitation is concentrated in June, July, and August, resulting in high RHs in summer. However, the meteorological data revealed that the RH in winter was almost the same as in summer, which is rare in the absence of anthropogenic effects. The major cause of such high RH in winter could be the usage of heat-only boilers (HOBs) in Ulaanbaatar. Although HOBs account for only 14% of the PM emissions according to previous work (Oyunchimeg and Tsolmon, 2011), they generate and emit a large amount

of water vapor. One study reported that the secondary particle production effect strengthened when there was no rainfall and RH was kept within the range of 60-80%, resulting in a positive correlation between $PM_{2.5}$ concentration and RH (Zhang *et al.*, 2016). This was in good agreement in our study in that our RH data showed that on most days with high $PM_{2.5}$ concentrations, the RH was between 60% and 80%.

We used LIDAR measurements combined with radiosonde data to observed the characteristic seasonal variations in the temperature inversion and mixed layers.
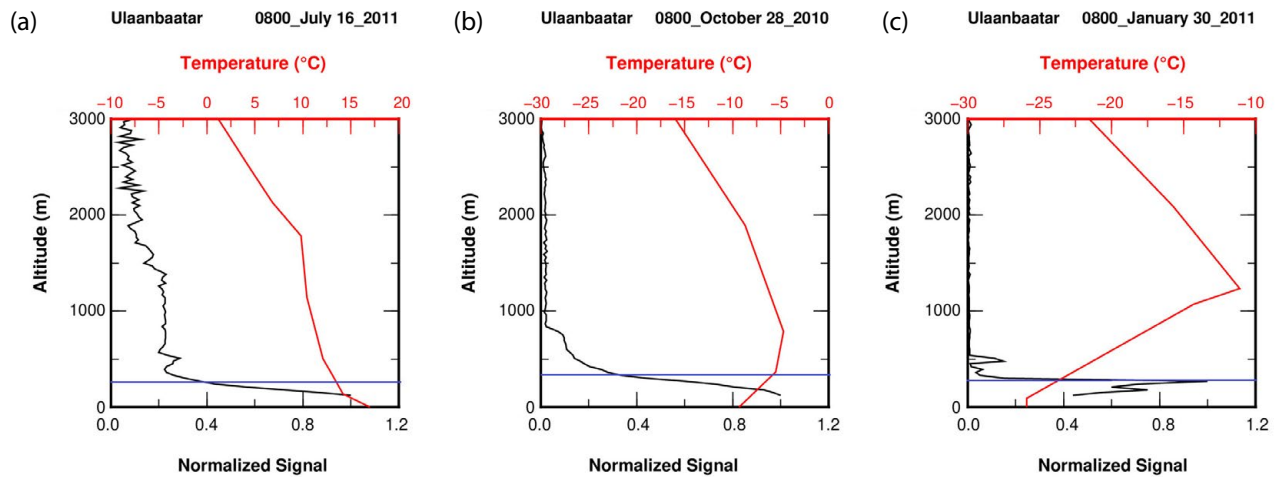
Fig. 7. Normalized LIDAR signal (black) and temperature (red) measured by the radiosonde at 08:00 LST on (a) July 16, 2011, (b) October 28, 2010 and (c) January 30, 2011. The blue line in three panels indicates the height of the mixed layer determined with the wavelength covariance transform method.
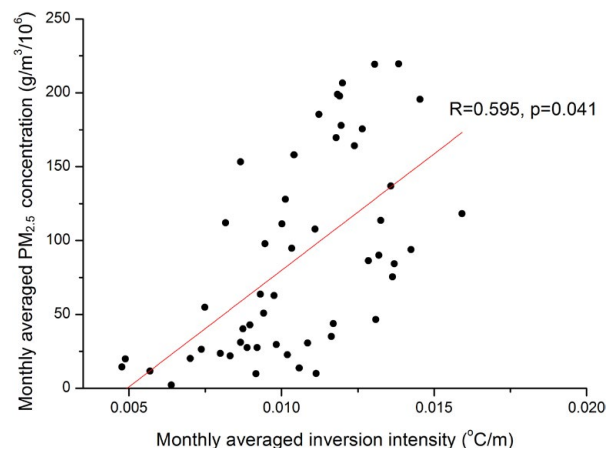

Fig. 8. Correlation between the monthly mean inversion intensity and monthly mean $PM_{2.5}$ concentration from March 2008 to December 2016. The inversion intensity was calculated as the quotient between the temperature inversion ΔT and inversion height Δh within 500-600 m (~800 hPa) above the ground (~865 hPa).

After determining the mixed layer height using the wavelet covariance transforming method based on NIES LIDAR data, which was also used in our previous work (Wang *et al.*, 2017), we compared the temperature inversion layer height defined using radiosonde data and the mixed layer height. The diurnal development of the mixed layer had a maximum height of almost 2000 m on a typical sunny summer day (e.g., July 16, 2011) and there was no temperature inversion (Fig. 6a). Although no temperature inversion was mea-

sured in summer, an overlapping inversion layer was observed in autumn and winter. The inversion layer height was defined from the radiosonde data measured at 08:00 LST. On January 30, 2011, the inversion layer height was much higher than the mixed layer at 08:00 LST (Fig. 7). This is a typical phenomenon on sunny days in winter in Ulaanbaatar. The temperature inversion layer persisted throughout the day and capped the developing mixed layer. On October 28, 2010 (Fig. 6b), the inversion layer thickness at 08:00 LST was at approximately the same level as the daily maximum height of the mixed layer (~700 m) and was broken through by the developed mixed layer between 12:00 and 16:00 LST. Surface wind is weak and vertical convection is almost nonexistent in winter (November-February), as we mentioned in our previous study that during 2010-2011 winter, the surface wind velocity was lower than 4 m/s (Wang *et al.*, 2017). The daily average surface temperature from December to February in our study period was below $-20°C$ and did not exceed 0°C until late March. This stable urban atmosphere persisted throughout winter, allowing the overlapping inversion layer to prevail throughout the day. Figs. 6c and 7 show a good example of this. The maximum height of the mixed layer was below 300 m on January 30, 2011, while the thickness of the inversion layer at 08:00 LST exceeded 850 m. The diurnal mixed layer developed slightly but was suppressed by the thick, overlapping inversion layer, which could no longer be broken through. This resulted in a low daily maximum

height and entrapment of particulate air pollutants. Such a pattern of mixed and temperature inversion layers differs substantially from that in Beijing (Tang *et al.*, 2016), which is mainly because of the Siberian High that dominates Ulaanbaatar and surrounding areas from late October to early March. Radiative cooling is strengthened by Ulaanbaatar's basin-like terrain, which enhances the stability of the urban atmosphere.

The thickness of the temperature inversion layer in Ulaanbaatar typically ranged from 500 to 700 m in December and January (Figs. 5 and 7), which was thicker than the mixed layer height in this period (<500 m). The result is comparable to the December average (~650 m) from 1981-2010 based on Ulaanbaatar radiosonde observations (Gerelchuluun and Ahn, 2014) and is in agreement with the value simulated using the Weather Research and Forecasting model (Ganbat and Baik, 2016). This phenomenon is unique among polluted cities worldwide, which usually have a higher mixed layer than temperature inversion layer. For instance, according to Yang *et al.* (2006), the monthly average height of the mixed layer in Shanghai varied from 500 to 700 m and the minimum value of the annual mixed layer was 525 m from 1990 to 2004. In addition, according to Xu *et al.* (2010), the mixed layer in Shanghai developed between 600 and 1300 m. Therefore, the much lower mixed layer and thicker temperature inversion layer in Ulaanbaatar have a characteristic restraining force on emitted particulate pollutants, which is somewhat similar to the relationship between the temperature inversion layer and surface ozone concentrations (Xu *et al.*, 1999).

Both the persistence time and intensity of the temperature inversion had seasonal variations that affected the concentration of particulate air pollutants. Fig. 8 shows the significant positive correlation (R = 0.595, p = 0.041) between the monthly averaged $PM_{2.5}$ and temperature inversion intensity $\left(\frac{\Delta T_{800}}{\Delta h_{800}}\right)$, which was calculated from March 2008 to December 2016. Meanwhile, the maximum values of $PM_{2.5}$, PM_{10}, ΔT, and Δh were observed in December and the maximum temperature inversion intensity was measured in January with a narrow margin over that for December (Table 1). During the research period, the temperature inversion layer became thicker and stronger every year from September to January, as the atmosphere became increasingly stable. As a result, emitted atmospheric particulate matter was concentrated at the ground level, which

resulted in severe particulate air pollution.

Previous research has indicated that the $PM_{2.5}$ concentration during winter in Ulaanbaatar exhibits hourly variations, where concentrations are higher at night and $\sim12:00$ LST and become weaker in the morning and afternoon (Mori *et al.*, 2012). Because the radiosonde data used in our study was collected at 08:00 LST, the $PM_{2.5}$ data we included in our comparison were also collected at that time of day. Although the 24-h average $PM_{2.5}$ concentration was much greater than that measured at 08:00 LST, it was still strongly correlated with temperature inversion intensity.

The only parameter in Ulaanbaatar that was substantially higher level than in Shanghai was the $PM_{2.5}/PM_{10}$ ratio (Table 2). The winter $PM_{2.5}/PM_{10}$ ratio in Shanghai is usually between 0.5-0.7, while that in Ulaanbaatar is 0.8 ± 0.07 (Nishikawa *et al.*, 2015; Allen *et al.*, 2013). There are several reasons to this phenomenon, and one of them might be the difference between the main emission sources among two cities. Generally, anthropogenic sources involving high temperature processes, such as coal combustion and vehicle exhaust, can produce fine particles (Morawska *et al.*, 2008). In the other hand, natural and anthropogenic mechanical processes, such as grinding, mining, construction, wear and tear of materials, and dust resuspension, contribute to the coarse fraction mode (Morawska *et al.*, 2008). Actually, the proportion of coal combustion among the emission sources in Ulaanbaatar is quite different from Shanghai. According to previous study, 64% of PM emissions from coal-fired sources in Ulaanbaatar are from households (Oyunchimeg and Tsolmon, 2011). Conversely, it is reported that among the local sources in Shanghai, mobile sources such as vehicles, ships, and aircrafts account for 29.2%, industrial production accounts for 28.9%, and coal combustion accounts for only 13.5% (Shanghai Environmental Protection Bureau, 2015). Since the concentration of $PM_{2.5}$ in Ulaanbaatar shows similar range of value with Shanghai, the industrial activities and ships, aircrafts that are ubiquitous in Shanghai but relatively infrequent in Ulaanbaatar, might be the reason to generate abundant $PM_{10-2.5}$, resulting in a decreased $PM_{2.5}/PM_{10}$ ratio. Besides, as a coastal city, Shanghai has relatively higher concentration of sea salt particles in its atmosphere, and occasionally receives long-range-transport floating dust from northern China, which could also increase $PM_{10-2.5}$ concentrations. On the other hand, Ulaanbaatar receives few

external transported particles in winter. In general, the difference of emission sources, anthropogenic activities, and geographic location between Ulaanbaatar and Shanghai could probably be the main reason of the difference of $PM_{2.5}/PM_{10}$ ratio.

5. CONCLUSIONS

We investigated the annual variations in $PM_{2.5}$, PM_{10}, visibility, and RH from March 2008 to April 2014 in Ulaanbaatar, Mongolia, using meteorological data. Their significant seasonal variations matched the results of our previous work, indicating that the particulate air pollution episode observed in 2010 was not an isolated case, but rather part of a regular pattern that has occurred every winter in recent years. By calculating the temperature inversion layer thickness and intensity from radiosonde data for 2008-2016, we elucidated the timing of the beginning and end of the temperature inversion layer that capped the urban area of Ulaanbaatar every winter, and found a strong correlation between the temperature inversion intensity and $PM_{2.5}$ concentrations. Based on the LIDAR and radiosonde data analysis, the meteorological and geographical characteristics of Ulaanbaatar lead to a unique urban atmospheric environment in midwinter, with a thick temperature inversion layer ($> 500\,m$) that overlays a weak, thin mixed layer ($< 300\,m$) during daytime. As a topic for future research, local radiosonde measurements at 1~2 hour intervals on sunny days during midwinter would help verify these results. Although Ulaanbaatar had the same $PM_{2.5}$ concentrations as Beijing and Shanghai, the winter $PM_{2.5}/PM_{10}$ ratio in Ulaanbaatar was higher than that of Shanghai. As part of the meteorological characteristics of Ulaanbaatar, the strong temperature inversion layer to some extent strengthened particulate air pollution in the urban area and should be examined further in future studies aiming to ameliorate urban particulate air pollution in Ulaanbaatar.

ACKNOWLEDGEMENT

REFERENCES

Abres, A.F., Ajero, M., Fabian, H., Ramirez, N. (2006) Country Synthesis Report on Urban Air Quality Management. The Asian Development Bank, Mongolia, 20p.

Allen, R., Gombojav, E., Batdorj, B., Tsogbaatar, B., Oyuntogus, L., Amram, O., Takaro, T., Janes, C. (2013) An assessment of air pollution and its attributable mortality in Ulaanbaatar, Mongolia. Air Quality, Atmosphere, and Health 6, 137-150.

Amarsaikhan, D., Blotevogel, H.H., Ganzorig, M., Moon, T.H. (2009) Applications of remote sensing and geographic information systems for urban land-cover change studies in Mongolia. Geocarto International 24(4), 257-271.

Davy, P.K., Gunchin, G., Markwitz, A., Trompetter, W., Barry, B., Shagjjamba, D., Lodoysamba, S. (2011) Air particulate matter pollution in Ulaanbaatar, Mongolia: determination of composition, source contributions and source locations. Atmospheric Pollution Research 2, 126-137.

Enkhbayar, Ts. (2014) Ger district and its development potentials in Mongolia, Fourth regional workshop on integrated resource management in Asian cities: The Urban Nexus, Ulaanbaatar, Mongolia, November 5-7, 2014.

Ganbat, G., Baik, J. (2016) Wintertime winds in and around the Ulaanbaatar Metropolitan Area in the presence of a temperature inversion. Asia-Pacific Journal of the Atmospheric Sciences 52(3), 309-325.

Gerelchuluun, B., Ahn, J.B. (2014) Air temperature distribution over Mongolia using dynamical downscaling and statistical correction. International Journal of Climatology 34, 2464-2476.

Guttikunda, S.K. (2007) Urban air pollution analysis for Ulaanbaatar, Mongolia. Consultation report. The World Bank, Washington, D.C., 120p.

Matsumiya, Y. (2015) On the urbanization of Ulaanbaatar: with special reference to the Ger areas. Research Journal of Graduate Students of Letters 43, Meiji University, 73-94. (in Japanese)

Morawska, L., Keogh, D.U., Thomas, S.B., Mengersen, K. (2008) Modality in Ambient Particle Size Distributions and its Potential as a Basis for Developing Air Quality Regulation. Atmospheric Environment 42, 1617-1628.

Mori, I., Yamazaki, M., Batdorj, D., Takahashi, A., Nishikawa, M., Matsui, I., Shimizu, A., Takahashi, K. (2012) Characteristics of Wintertime Airborne Particulate Matter in Ulaanbaatar. Proceedings of the 53rd Annual Meeting of Japan Society of Atmospheric Environment, Yokohama, 492. (in Japanese)

Nishikawa, M., Matsui, I., Batdorj, D., Jugder, D., Mori, I., Shimizu, A., Sugimoto, N., Takahashi, K. (2011) Chemical composition of urban airborne particulate matter in Ulaan-

baatar. Atmospheric Environment 45, 5710-5715.

Nishikawa, M., Matsui, I., Mori, I., Batdorj, D., Sarangerel, E., Ohnishi, K., Shimizu, A., Sugimoto, N. (2015) Chemical characteristics of airborne particulate matter during the winter season in Ulaanbaatar. Earozoru Kenkyu 30, 126-133.

Nyamtseren, L. (2009) Air Pollution Issues of UB City and Some Evaluations of Coming Activities. Mongolian Development Institute, Ulaanbaatar.

Oyunchimeg, D., Tsolmon (2011) Emission inventory of coal fired emission sources in Capital city, Mongolia. Papers in Meteorology and Hydrology 32/8, 162-169.

Oyunchimeg, U., Burmaa, B. (2005) Study on Ulaanbaatar city air pollution influence on birth defects. Mongolian Medicine 4, 32-35.

Shanghai Environmental Protection Bureau, 2015, http://www.sepb.gov.cn/fa/cms/shhj/shhj2272/shhj2159/2015/01/88463.htm. (in Chinese)

Sugimoto, N., Nishizawa, T., Liu, X., Matsui, I., Shimizu, A., Zhang, Y., Kim, Y.J., Li, R., Liu, J. (2009) Continuous observations of aerosol profiles with a two-wavelength Mie-scattering lidar in Guangzhou in PRD2006. Journal of Applied Meteorology and Climatology 48, 1822-1830.

Tang, G., Zhang, J., Zhu, X., Song, T., Munkel, C., Hu, B., Schafer, K., Liu, Z., Zhang, J., Wang, L., Xin, J., Suppan, P., Wang, Y. (2016) Mixing layer height and its implications for air pollution over Beijing, China. Atmospheric Chemistry and Physics 16, 2459-2475.

Wang, J., Hu, Z., Chen, Y., Chen, Z., Xu, S. (2013) Contamination characteristics and possible sources of PM_{10} and $PM_{2.5}$ in different functional areas of Shanghai, China. Atmospheric Environment 68, 221-229.

Wang, M., Kai, K., Sugimoto, N., Jin, Y., Batdorj, D. (2017) Air particulate pollution in Ulaanbaatar, Mongolia: Variation in atmospheric conditions from autumn to winter. Science Online Letters on the Atmosphere 13, 90-95, doi:10.2151/sola.2017-017.

World Bank (2009) Mongolia, Air Pollution in Ulaanbaatar: Initial Assessment of Current Situation and Effects of Abatement Measures. The World Bank, Washington, D.C., 146p.

World Bank (2010) Enhancing policies and practices for Ger area development in Ulaanbaatar. The World Bank, Washington, D.C., 127p.

Xu, J., Geng, F., Zhen, C., Gao, W. (2010) Aerosol scattering coefficients and the factors affecting them in Shanghai Pudong. Acta Scientiae Circumstantiae 30(1), 211-216. (in Chinese)

Xu, J., Zhu, Y., Li, J. (1999) Case studies on the processes of surface ozone pollution in Shanghai. Journal of the Air & Waste Management Association 49(6), 716-724.

Yang, Y., Tan, J., Zheng, Y., Cheng, S. (2006) Study on the atmospheric stabilities and the thickness of atmospheric mixed layer during recent 15 years in Shanghai. Scientia Meteorologica Sinica 26(5), 536-541. (in Chinese)

Yonemochi, S., Chen, X., Miao, P., Lu, S., Oh, K., Umezawa, N. (2013) Characterization of high concentration of $PM_{2.5}$ and PM1 collected in Beijing in January. Journal of Japan Society for Atmospheric Environment 48(3), 140-144. (in Japanese)

Zhang, S., Han, L., Zhou, W., Zheng, X. (2016) Relationships between fine particulate matter ($PM_{2.5}$) and meteorological factors in winter at typical Chinese cities. Acta Ecologica Sinica, 36(24), 7897-7907. (in Chinese)